Antikaon condensation and the metastability of protoneutron stars

Sarmistha Banik and Debades Bandyopadhyay
Saha Institute of Nuclear Physics, 1/AF Bidhannagar, Calcutta 700 064, India
(Received 5 September 2000; published 9 February 2001)

We investigate the condensation of $\bar{K}^0$ mesons along with K^- condensation in neutrino-trapped matter with and without hyperons. Calculations are performed in the relativistic mean field models in which both the baryon-baryon and (anti)kaon-baryon interactions are mediated by meson exchange. In the neutrino-trapped matter relevant to protoneutron stars, the critical density of K^- condensation is shifted considerably to higher density whereas that of $\bar{K}^0$ condensation is shifted slightly to higher density with respect to that of the neutrino-free case. The onset of K^- condensation always occurs earlier than that of $\bar{K}^0$ condensation. A significant region of maximum mass protoneutron stars is found to contain $\bar{K}^0$ condensate for larger values of the antikaon potential. With the appearance of $\bar{K}^0$ condensation, there is a region of symmetric nuclear matter in the inner core of a protoneutron star. We note that the gross properties of the protoneutron stars are significantly affected by the antikaon condensation for larger values of the antikaon potential. It is found that the maximum mass of a protoneutron star containing K^- and $\bar{K}^0$ condensate is greater than that of the corresponding neutron star. We reexamine the implication of this scenario in the context of the metastability of protoneutron stars and their evolution to low mass black holes.

DOI: 10.1103/PhysRevC.63.035802 PACS number(s): 26.60.+c, 21.65.+f, 97.60.Jd, 95.30.Cq

I. INTRODUCTION

It was suggested by Woosley and Weaver [1] that progenitor stars heavier than $\sim 25 M_\odot$ would collapse into black holes. In this scenario, stars first explode, then exhibit light curves of type II supernova, and return matter to the galaxy before going into black holes. This issue got impetus after the explosion of SN 1987A. One of the revealing features of SN 1987A is that a neutrino was observed in Kamiokande II at the 12th second. So far there has been no observation of a pulsar within it. Moreover, the light curve fades away, leading to speculation that the compact object in SN 1987A has collapsed into a low mass black hole. If this picture of low mass black hole formation is true for SN 1987A, the newly born hot and neutrino-rich star, called a protoneutron star, was stable over 12 s or more before collapsing into a black hole.

In recent years, there have been several works by various groups [2–4] to understand what is the mechanism behind the stability of protoneutron stars for short times. In the ''conventional'' scenario where (proto)neutron stars are made up of nucleons and leptons, the protoneutron star has a slightly smaller maximum mass than that of the neutron star. The ''window'' of maximum masses is very small in this case. However, the scenario dramatically changes with the formation of K^- condensation in dense matter as found in previous calculations [2–4]. They showed that leptons could stabilize a much larger maximum mass for a protoneutron star in the presence of K^- condensation during the evolution. In the following paragraph, we briefly review the previous calculations of K^- condensation in dense matter relevant to (proto)neutron stars.

With the pioneering work of Kaplan and Nelson [5], considerable interest has been generated in the study of antikaon ($\bar{K}$) condensation in dense matter in recent years. In a chiral $SU(3)_L \times SU(3)_R$ model, baryons directly couple with (anti)kaons. The effective mass m_K^* of antikaons decreases with density because of the strongly attractive K^--baryon interaction in dense matter. Consequently, the in-medium energy (ω_{K^-}) of K^- mesons in the zero-momentum state also decreases with density. The *s*-wave K^- condensation sets in when ω_{K^-} equals the chemical potential of the K^- meson. Later, this chiral model was adopted by other groups to study K^- condensation in the core of neutron stars [6–8] using kaon-nucleon scattering data [9,10] and K^- atomic data [11]. On the other hand, K^- condensation has been studied in a different kind of model which is an extension of the Walecka model [12–15]. In this model, kaons interact with baryons through the exchange of mesons. It is found that the threshold density of K^- condensation in various calculations depends on the equation of state and parameters, in particular on the antikaon optical potential. The net effect of K^- condensation in neutron star matter is that K^- condensate replaces electrons in maintaining charge neutrality and softens the equation of state. As a result of the softening of the equation of state, the masses of the stars are reduced in the presence of K^- condensate [7,12–15]. It was also found that in the presence of hyperons, K^- condensation was delayed to higher density and might not even exist in maximum mass stars. Protoneutron stars with K^- condensate were studied by various groups [2,4,7,16] and shown to have maximum masses larger than those of cold neutron stars—a reversal of the ''conventional scenario.'' Theoretical studies based on the above-mentioned models [9,13,14] and also on the Nambu–Jona-Lasinio model [17] yield a repulsive optical potential for K^+ in the nuclear medium. Therefore, K^+ condensation may not be a possibility in (proto)neutron stars.

In a recent calculation [18], the formation of $\bar{K}^0$-meson condensation in neutron stars has been investigated within a relativistic mean field approach [19] where the interaction between the baryons and antikaons is generated by the exchange of σ, ω, and ρ mesons. It is found that the ρ-meson field is repulsive for the K^- meson, whereas it is attractive for the $\bar{K}^0$ meson which is an isodoublet partner of the K^-

meson. Consequently, the in-medium energy ($\omega_{\bar{K}^0}$) of the $\bar{K}^0$ meson is lowered compared with that of the K^- meson, thereby making $\bar{K}^0$ meson condensation more favorable in neutron star matter. The critical density for *s*-wave neutral $\bar{K}^0$ meson condensation is governed by the condition $\omega_{\bar{K}^0}=0$. It was found that the critical densities for K^- and $\bar{K}^0$ condensation depended sensitively on the choice of the antikaon optical potential depth and more strongly on the nuclear equation of state (EOS). The threshold density of $\bar{K}^0$ condensation always lies above that of K^- condensation. With the appearance of K^- and $\bar{K}^0$ condensate, the overall equation of state becomes softer than the situation without antikaon condensation, leading to a reduction in the maximum masses of neutron stars. With the onset of only K^- condensation, the proton fraction rises dramatically and even crosses the neutron fraction at some density because of charge neutrality. With the onset of $\bar{K}^0$ condensation, there is a competition in the formation of K^--p and $\bar{K}^0$-n pairs, resulting in a perfectly symmetric matter for nucleons and antikaons inside neutron stars. In the presence of hyperons, it was found that the formation of antikaon condensation was delayed to higher densities and the maximum mass neutron star contained $\bar{K}^0$ condensate for larger values of the antikaon potential depth [18].

So far, there has been no calculation of $\bar{K}^0$ condensation and its impact on the gross properties of protoneutron stars. In this paper, we investigate the effect of antikaon condensation with emphasis on the role of $\bar{K}^0$ condensate to determine the composition and structure of protoneutron stars in the standard meson exchange model [19]. In this calculation, we adopt the usual relativistic mean field Lagrangian [14,15,18] for baryons interacting via meson exchanges. Also, we include the self-interaction of the scalar meson and the nonlinear ω meson term in the calculation [14]. The (anti)kaon-baryon interaction is treated on the same footing as the baryon-baryon interaction. The Lagrangian density for (anti)kaons is taken from Refs. [15,18]. We shall show within this model that $\bar{K}^0$ condensate may also exist inside a protoneutron star and has a significant influence on the star's properties and evolution.

The paper is organized as follows. In Sec. II we describe the relativistic mean field (RMF) model of strong interactions. The relevant equations for (proto)neutron star matter with antikaon condensates are summarized in this model. In Sec. III the parameters of the model are discussed and results of antikaon condensates in (proto)neutron star matter are presented. Section IV is devoted to the summary and conclusions.

II. FORMALISM

We describe the charge-neutral and beta-equilibrated matter consisting of baryons, electrons, muons, and electron-type neutrinos in the presence of antikaon condensates. The matter inside a protoneutron star is highly degenerate. The chemical potentials of its constituents are a few hundreds of MeV, whereas the central temperature of the star is a few tens of MeV. Neglecting the finite temperature effect will have little effect on the gross properties of the star. However, the compositional changes caused by the trapped neutrinos may induce relatively larger changes in the formation of antikaon condensation [4]. Therefore, we perform zero-temperature calculations of (proto)neutron stars in the presence of antikaon condensation. The starting point in the present approach is a relativistic field theoretical model of baryons and (anti)kaons interacting by the exchange of scalar σ, isoscalar vector ω, and vector isovector ρ mesons and two additional hidden-strangeness mesons, the scalar meson $f_0(975)$ (denoted hereafter as σ^*) and the vector meson $\phi(1020)$, to allow for the hyperon-hyperon interaction [14,20]. The total Lagrangian density consists of the baryonic, kaonic, and leptonic parts, i.e., $\mathcal{L}=\mathcal{L}_B+\mathcal{L}_K+\mathcal{L}_l$. Here we consider all the species of the baryon octet $B\equiv\{n,p,\Lambda,\Sigma^+,\Sigma^-,\Sigma^0,\Xi^-,\Xi^0\}$. The baryonic Lagrangian density is given by

$$\mathcal{L}_B=\sum_B \bar{\psi}_B\left(i\gamma_\mu\partial^\mu-m_B+g_{\sigma B}\sigma-g_{\omega B}\gamma_\mu\omega^\mu-\frac{1}{2}g_{\rho B}\gamma_\mu\boldsymbol{\tau}_B\cdot\boldsymbol{\rho}^\mu\right)\psi_B$$
$$+\frac{1}{2}(\partial_\mu\sigma\partial^\mu\sigma-m_\sigma^2\sigma^2)-U(\sigma)-\frac{1}{4}\omega_{\mu\nu}\omega^{\mu\nu}+\frac{1}{2}m_\omega^2\omega_\mu\omega^\mu-\frac{1}{4}\boldsymbol{\rho}_{\mu\nu}\cdot\boldsymbol{\rho}^{\mu\nu}+\frac{1}{2}m_\rho^2\boldsymbol{\rho}_\mu\cdot\boldsymbol{\rho}^\mu+\mathcal{L}_{YY}. \quad (1)$$

Here ψ_B denotes the Dirac spinor for baryon B with vacuum mass m_B and isospin operator $\boldsymbol{\tau}_B$. The scalar self-interaction term [21] is

$$U(\sigma)=\frac{1}{3}g_2\sigma^3+\frac{1}{4}g_3\sigma^4. \quad (2)$$

The Lagrangian density ($\mathcal{L}_{YY}$) responsible for the hyperon-hyperon interaction is given by

$$\mathcal{L}_{YY}=\sum_B \bar{\psi}_B(g_{\sigma^* B}\sigma^*-g_{\phi B}\gamma_\mu\phi^\mu)\psi_B$$
$$+\frac{1}{2}(\partial_\mu\sigma^*\partial^\mu\sigma^*-m_{\sigma^*}^2\sigma^{*2})$$
$$-\frac{1}{4}\phi_{\mu\nu}\phi^{\mu\nu}+\frac{1}{2}m_\phi^2\phi_\mu\phi^\mu. \quad (3)$$

The Lagrangian density for (anti)kaons in the minimal coupling scheme is given by [15]

$$\mathcal{L}_K = D_\mu^* \bar{K} D^\mu K - m_K^{*2} \bar{K} K, \tag{4}$$

where the covariant derivative $D_\mu = \partial_\mu + i g_{\omega K} \omega_\mu + i g_{\phi K} \phi_\mu + i g_{\rho K} \boldsymbol{\tau}_K \cdot \boldsymbol{\rho}_\mu$. The isospin doublet for kaons is denoted by $K \equiv (K^+, K^0)$ and that for antikaons is $\bar{K} \equiv (K^-, \bar{K}^0)$. The effective mass of (anti)kaons in this minimal coupling scheme is given by

$$m_K^* = m_K - g_{\sigma K} \sigma - g_{\sigma^* K} \sigma^*, \tag{5}$$

where m_K is the bare kaon mass. In the mean field approximation (MFA) [19] adopted here, the meson fields are replaced by their expectation values. Only the timelike components of the vector fields and the isospin three-component of ρ-meson field have nonvanishing values in a uniform and static matter. The mean meson fields are denoted by σ, σ^*, ω_0, ϕ_0, and ρ_{03}.

The dispersion relation representing the in-medium energies of $\bar{K} \equiv (K^-, \bar{K}^0)$ for s-wave ($\mathbf{k} = 0$) condensation is given by

$$\omega_{K^-, \bar{K}^0} = m_K^* - g_{\omega K} \omega_0 - g_{\phi K} \phi_0 \mp \frac{1}{2} g_{\rho K} \rho_{03}, \tag{6}$$

where the isospin projection $I_{3\bar{K}} = \mp 1/2$ for the mesons K^- ($-$ sign) and $\bar{K}^0$ ($+$ sign) are explicitly written in the expression. Since the σ and ω fields generally increase with density and both terms containing σ and ω fields in Eq. (6) are attractive for antikaons, the in-medium energies of $\bar{K}$ decrease in the nuclear medium. On the other hand, in nucleon-only matter, $\rho_{03} \equiv n_p - n_n$ (n_p and n_n are the proton and neutron densities) is negative; thus the ρ-meson field favors the formation of $\bar{K}^0$ condensation over that of K^- condensation. In hyperon matter, the repulsive ϕ-meson term may delay the onset of antikaon condensation [14]. The in-medium energies of kaons $K \equiv (K^+, K^0)$ are given by

$$\omega_{K^+, K^0} = m_K^* + g_{\omega K} \omega_0 + g_{\phi K} \phi_0 \pm \frac{1}{2} g_{\rho K} \rho_{03}. \tag{7}$$

It is to be noted here that kaon condensation may be impossible in neutron star matter because the ω-meson term is repulsive for kaons and dominates over the attractive σ-meson term at higher densities. However, the attractive ϕ meson term may decrease kaon energies in the presence of hyperons [14].

The meson field equations in the presence of baryons and antikaon condensates are derived from Eqs. (1)–(4) as

$$m_\sigma^2 \sigma = -\frac{\partial U}{\partial \sigma} + \sum_B g_{\sigma B} n_B^S + g_{\sigma K} \sum_{\bar{K}} n_{\bar{K}}, \tag{8}$$

$$m_{\sigma^*}^2 \sigma^* = \sum_B g_{\sigma^* B} n_B^S + g_{\sigma^* K} \sum_{\bar{K}} n_{\bar{K}}, \tag{9}$$

$$m_\omega^2 \omega_0 = \sum_B g_{\omega B} n_B - g_{\omega K} \sum_{\bar{K}} n_{\bar{K}}, \tag{10}$$

$$m_\phi^2 \phi_0 = \sum_B g_{\phi B} n_B - g_{\phi K} \sum_{\bar{K}} n_{\bar{K}}, \tag{11}$$

$$m_\rho^2 \rho_{03} = \sum_B g_{\rho B} I_{3B} n_B + g_{\rho K} \sum_{\bar{K}} I_{3\bar{K}} n_{\bar{K}}. \tag{12}$$

Here the scalar and number densities of baryon B are, respectively,

$$n_B^S = \frac{2J_B + 1}{2\pi^2} \int_0^{k_{F_B}} \frac{m_B^*}{(k^2 + m_B^{*2})^{1/2}} k^2 dk, \tag{13}$$

$$n_B = (2J_B + 1) \frac{k_{F_B}^3}{6\pi^2}, \tag{14}$$

with effective baryonic mass $m_B^* = m_B - g_{\sigma B} \sigma - g_{\sigma^* B} \sigma^*$, Fermi momentum k_{F_B}, spin J_B, and isospin projection I_{3B}. Note that for s-wave $\bar{K}$ condensation, the scalar and vector densities of antikaons are same and those are given by [15]

$$n_{K^-, \bar{K}^0} = 2 \left(\omega_{K^-, \bar{K}^0} + g_{\omega K} \omega_0 + g_{\phi K} \phi_0 \pm \frac{1}{2} g_{\rho K} \rho_{03} \right) \bar{K} K = 2 m_K^* \bar{K} K. \tag{15}$$

The total energy density $\varepsilon = \varepsilon_B + \varepsilon_l + \varepsilon_{\bar{K}}$ has contributions from baryons, leptons, and antikaons. The baryonic plus leptonic energy density is

$$\begin{aligned} \varepsilon_B + \varepsilon_l = {} & \frac{1}{2} m_\sigma^2 \sigma^2 + \frac{1}{3} g_2 \sigma^3 + \frac{1}{4} g_3 \sigma^4 + \frac{1}{2} m_{\sigma^*}^2 \sigma^{*2} + \frac{1}{2} m_\omega^2 \omega_0^2 \\ & + \frac{1}{2} m_\phi^2 \phi_0^2 + \frac{1}{2} m_\rho^2 \rho_{03}^2 + \sum_B \frac{2J_B + 1}{2\pi^2} \\ & \times \int_0^{k_{F_B}} (k^2 + m_B^{*2})^{1/2} k^2 dk + \sum_l \frac{1}{\pi^2} \\ & \times \int_0^{K_{F_l}} (k^2 + m_l^2)^{1/2} k^2 dk + \frac{\mu_{\nu_e}^4}{8\pi^2}, \end{aligned} \tag{16}$$

where l goes over electrons and muons. The last term corresponds to the energy density of neutrinos as required in protoneutron star matter. The energy density for antikaons is

$$\varepsilon_{\bar{K}} = m_K^* (n_{K^-} + n_{\bar{K}^0}). \tag{17}$$

Since antikaons form s-wave Bose condensates, they do not directly contribute to the pressure so that the pressure is due to baryons and leptons only:

$$P=-\frac{1}{2}m_\sigma^2\sigma^2-\frac{1}{3}g_2\sigma^3-\frac{1}{4}g_3\sigma^4-\frac{1}{2}m_{\sigma*}^2\sigma^{*2}+\frac{1}{2}m_\omega^2\omega_0^2$$
$$+\frac{1}{2}m_\phi^2\phi_0^2+\frac{1}{2}m_\rho^2\rho_{03}^2+\frac{1}{3}\sum_B\frac{2J_B+1}{2\pi^2}\int_0^{k_{F_B}}\frac{k^4dk}{(k^2+m_B^{*2})^{1/2}}$$
$$+\frac{1}{3}\sum_l\frac{1}{\pi^2}\int_0^{K_{F_l}}\frac{k^4dk}{(k^2+m_l^2)^{1/2}}+\frac{\mu_{\nu_e}^4}{24\pi^2}. \quad (18)$$

Here, the last term is the contribution of neutrinos to the pressure. The pressure due to antikaons is contained entirely in the meson fields via their field equations (8)–(12).

At the interior of (proto)neutron stars, baryons are in chemical equilibrium under weak processes. Therefore the chemical potentials of baryons and leptons are governed by the equilibrium conditions

$$\mu_i=b_i\mu_n-q_i(\mu_e-\mu_{\nu_e}), \quad (19)$$

where μ_i, μ_n, μ_e, and μ_{ν_e} are, respectively, the chemical potentials of the ith baryon, neutrons, electrons, and neutrinos, with $\mu_i=(k_{F_i}^2+m_i^{*2})^{1/2}+g_{\omega i}\omega_0+g_{\phi i}\phi_0+I_{3i}g_{\rho i}\rho_{03}$, and b_i and q_i are the baryon and electric charge of the ith baryon, respectively. In neutron stars, electrons are converted to muons by $e^-\rightarrow\mu^-+\bar{\nu}_\mu+\nu_e$ when the electron chemical potential becomes equal to the muon mass. Therefore, we have $\mu_e=\mu_\mu$ in a neutron star. On the other hand, muons are absent in a protoneutron star. With the onset of $\bar{K}$ condensation, various strangeness changing processes may occur in (proto)neutron stars such as $N\rightleftharpoons N+\bar{K}$ and $e^-\rightleftharpoons K^-+\nu_e$, where $N\equiv(n,p)$ and $\bar{K}\equiv(K^-,\bar{K}^0)$ denote the isospin doublets for nucleons and antikaons, respectively. The requirement of chemical equilibrium yields

$$\mu_n-\mu_p=\mu_{K^-}=\mu_e-\mu_{\nu_e}, \quad (20)$$

$$\mu_{\bar{K}^0}=0, \quad (21)$$

where μ_{K^-} and $\mu_{\bar{K}^0}$ are, respectively, the chemical potentials of K^- and $\bar{K}^0$. The above conditions determine the onset of antikaon condensation in neutrino-trapped matter. When the effective energy of the K^- meson (ω_{K^-}) is equal to its chemical potential (μ_{K^-}) which, in turn, is equal to $\mu_e-\mu_{\nu_e}$, a K^- condensate is formed. Similarly, $\bar{K}^0$ condensation is formed when its in-medium energy satisfies the condition $\omega_{\bar{K}^0}=\mu_{\bar{K}^0}=0$. It is to be noted here that the neutrino chemical potential (μ_{ν_e}) is zero for the neutrino free case corresponding to neutron stars. For (proto)neutron star matter we need to include also the charge neutrality condition, which in the presence of antikaon condensate is expressed as

$$\sum_i q_in_i-n_{K^-}-n_e-n_\mu=0, \quad (22)$$

where q_i and n_i are the electric charge and density of the ith baryon, respectively. The other constraint in protoneutron stars is the number of leptons per baryon. Gravitational core collapse calculations of massive stars indicate that the lepton fraction at the onset of trapping is $Y_{L_e}=Y_e+Y_{\nu_e}\simeq0.4$ and it is conserved on a dynamical time scale [4].

TABLE I. The nucleon-meson coupling constants in the GM1 set are taken from Ref. [22]. In this relativistic model, the baryons interact via nonlinear σ-meson and linear ω-meson exchanges. The coupling constants are obtained by reproducing the nuclear matter properties of the binding energy $E/B=-16.3$ MeV, baryon density $n_0=0.153$ fm^{-3}, asymmetry energy coefficient $a_{\rm asy}=32.5$ MeV, incompressibility $K=300$ MeV, and effective nucleon mass $m_N^*/m_N=0.70$. The hadronic masses are $m_N=938$ MeV, $m_\sigma=550$ MeV, $m_\omega=783$ MeV, and $m_\rho=770$ MeV. The parameter set TM1 is obtained from Ref. [30] which incorporates nonlinear exchanges in both σ and ω mesons. The nuclear matter properties in the TM1 set are $E/B=-16.3$ MeV, $n_0=0.145$ fm^{-3}, $a_{\rm asy}=36.9$ MeV, $K=281$ MeV, and $m_N^*/m_N=0.634$. All the hadronic masses in this model are same as GM1 except for the σ meson which is $m_\sigma=511.198$ MeV. All the parameters are dimensionless, except g_2 which is in fm^{-1}.

	$g_{\sigma N}$	$g_{\omega N}$	$g_{\rho N}$	g_2	g_3	g_4
GM1	9.5708	10.5964	8.1957	12.2817	-8.9780	−
TM1	10.0289	12.6139	4.6322	-7.2325	0.6183	71.3075

III. RESULTS AND DISCUSSION

In the effective field theoretic approach adopted here, we first consider nucleon-only matter where two distinct sets of coupling constants for nucleons and kaons associated with the exchange of σ, ω, and ρ mesons are required. The nucleon-meson coupling constants generated by reproducing the nuclear matter saturation properties are taken from Glendenning and Moszkowski [22]. This set is referred to as GM1 and is listed in Table I.

Now we determine the kaon-meson coupling constants. According to the quark model and isospin counting rule, the vector coupling constants are given by

$$g_{\omega K}=\frac{1}{3}g_{\omega N} \text{ and } g_{\rho K}=g_{\rho N}. \quad (23)$$

The scalar coupling constant is obtained from the real part of the K^- optical potential at normal nuclear matter density:

$$U_{\bar{K}}(n_0)=-g_{\sigma K}\sigma-g_{\omega K}\omega_0. \quad (24)$$

The negative sign in the vector meson potential is due to G parity. The critical density of $\bar{K}$ condensation should therefore strongly depend on the K^- optical potential.

It has been demonstrated in various calculations that antikaons feel an attractive potential in normal nuclear matter [10,23–26]. The analysis of K^- atomic data [24] in a hybrid model comprised of the relativistic mean field approach in the nuclear interior and a phenomenological density dependent potential at low density revealed that the real part of the antikaon optical potential could be as large as $U_{\bar{K}}=-180\pm20$ MeV at normal nuclear matter density and repulsive at

TABLE II. The coupling constants for antikaons ($\bar{K}$) to σ mesons, $g_{\sigma K}$, for various values of $\bar{K}$ optical potential depths $U_{\bar{K}}$ (in MeV) at the saturation density. The results are for the GM1 and TM1 set.

$U_{\bar{K}}$	-100	-120	-140	-160	-180
GM1	0.9542	1.6337	2.3142	2.9937	3.6742
TM1	0.2537	0.8384	1.4241	2.0098	2.5955

low density in accordance with the low density theorem. In the coupled channel calculation [25] for antikaons, the attractive antikaon potential depth was estimated to be $U_{\bar{K}} = -100$ MeV, whereas the chirally motivated coupled channel approach predicted a depth of $U_{\bar{K}} = -120$ MeV [26]. The wide range of values of the antikaon potential depth as found in various calculations may be attributed to the different treatments of $\Lambda(1405)$ resonance which is considered to be an unstable $\bar{K}N$ bound state just below the $K^- p$ threshold. Therefore, we determine the K-σ coupling constant $g_{\sigma K}$ from a set of values of $U_{\bar{K}}(n_0)$ starting from -100 MeV to -180 MeV. This is listed in Table II for the set GM1. Since the ω-meson potential for $\bar{K}$ in this model is $V_\omega^K(n_0) = -g_{\omega K}\omega_0 \approx -72$ MeV, a rather large sigma-kaon coupling constant of $g_{\sigma K} = 3.674$ is required to reproduce a depth of -180 MeV. It is to be noted that for this large depth, the value of the scalar coupling is similar to the prediction in the simple quark model, i.e., $g_{\sigma K} = g_{\sigma N}/3$. In an alternative approach the kaon-meson coupling constants were also determined from the *s*-wave kaon-nucleon (KN) scattering length [14,27,28].

We now present results for (proto)neutron star matter containing nucleons, leptons, and $\bar{K}$ condensates for the parameter set GM1 in Tables I and II. In Fig. 1, the scalar and vector potentials are displayed as a function of baryon density normalized to the equilibrium value of $n_0 = 0.153$ fm^{-3} with the K^- optical potential depth of $U_{\bar{K}}(n_0) = -160$ MeV for the neutrino-free (top panel) and neutrino-trapped (bottom panel) cases. In both cases, the scalar (σ) and vector (ω) potentials increase with density before the onset of antikaon condensation. In the neutrino-free case, two curves touch each other just at the onset of K^- condensation, whereas the curve of the vector (ω) potential crosses the curve of the scalar potential before the appearance of antikaon condensation in the neutrino-trapped case. After the formation of $\bar{K}$ condensates, the curves change slope; i.e., the rate of increase of the fields is altered with respect to the previous situations. With the appearance of $\bar{K}^0$ condensate, the isovector potential approaches zero with increasing density in the neutrino-free case, whereas it goes to zero and then bounces back for the neutrino-trapped case. It is found that the scalar potential for neutrino-free matter becomes larger after the onset of antikaon condensation than that of neutrino-trapped matter. It follows from Eq. (8) and this reasoning that the onset of $\bar{K}$ condensation is delayed to higher densities in neutrino-trapped matter. Though the vector potentials are comparable in both cases up to $\sim 2.5 n_0$, it

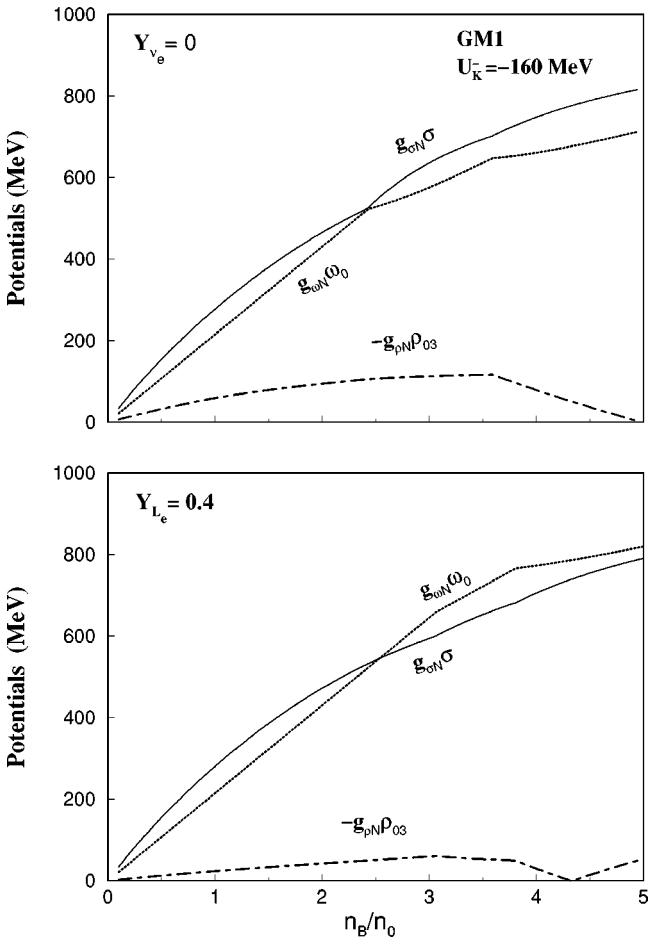

FIG. 1. The mean meson potentials versus the baryon density n_B/n_0 in the GM1 set for neutrino-free (top panel) and neutrino-trapped (bottom panel) nucleon-only star matter with the inclusion of antikaon, K^- and $\bar{K}^0$, condensation. The $\bar{K}$ optical potential depth is $U_{\bar{K}} = -160$ MeV at the normal nuclear matter density of $n_0 = 0.153$ fm^{-3}.

is higher for the neutrino-trapped case at higher densities. On the other hand, the isovector potential in neutrino-trapped matter is always smaller compared to that of neutrino-free matter. Those variations in the meson fields may be attributed to the different behavior of the source terms in the field equations of motion [Eqs. (8), (10), and (12)] and the composition of matter in two cases.

The effective mass ratio of antikaons, m_K^*/m_K, is shown in Fig. 2 as a function of normalized baryon density for $U_{\bar{K}} = -160$ MeV. The solid line represents the neutrino-free case, whereas the dotted line denotes the neutrino-trapped situation. It is found that the effective mass in neutrino-free matter is smaller than that of neutrino-trapped matter at higher densities. This may be attributed to the larger scalar potential at higher densities in the former case.

Figure 3 shows the *s*-wave antikaon condensation energies for neutrino-free and neutrino-trapped nuclear matter as a function of baryon density. The calculation is done with the antikaon potential depth of $U_{\bar{K}} = -160$ MeV. The solid lines correspond to the energy of the K^- meson, ω_{K^-}, whereas the dashed lines indicate that of the $\bar{K}^0$ meson, $\omega_{\bar{K}^0}$. Also, the

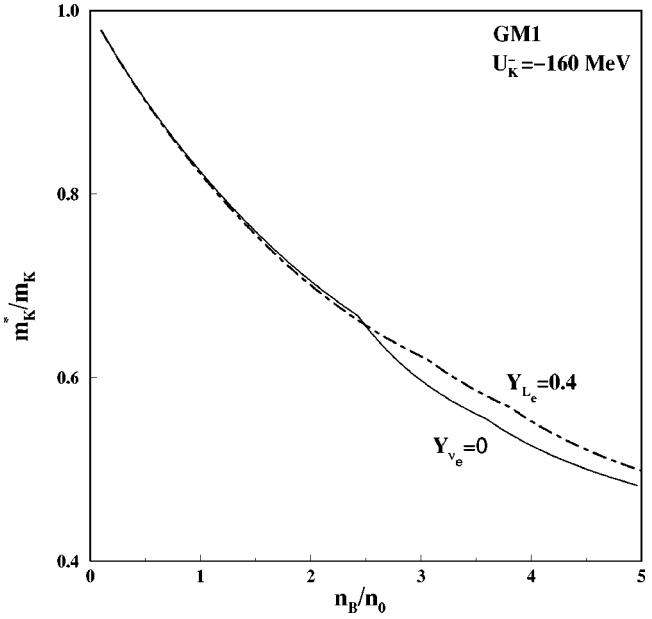

FIG. 2. The variation of the effective mass of (anti)kaons m_K^*/m_K as a function of baryon density n_B/n_0 for neutron star matter (solid line) and protoneutron star matter (dashed line) consisting of nucleons and antikaon condensates in the GM1 set. The $\bar{K}$ optical potential depth at normal nuclear matter density is $U_{\bar{K}}=-160$ MeV for this calculation.

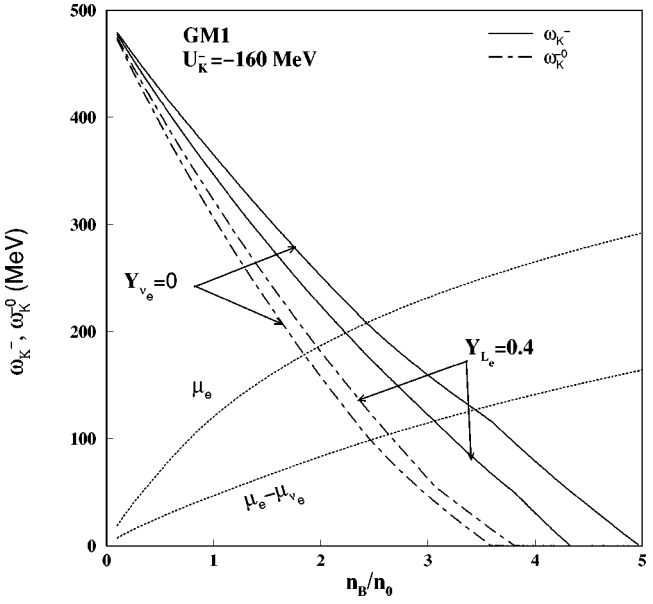

FIG. 3. The in-medium energy of K^- (solid lines) and $\bar{K}^0$ (dashed lines) versus baryon density for neutrino-free (-trapped) nucleon-only matter in the GM1 set. The electrochemical potential (μ_e) and the difference of the electrochemical potential and the neutrino chemical potential, i.e., $\mu_e-\mu_{\nu_e}$, are also shown in the figure. The $\bar{K}$ optical potential at normal nuclear matter density is $U_{\bar{K}}=-160$ MeV.

electron chemical potential (μ_e) for the neutrino-free case and the difference between electron and neutrino chemical potentials, $\mu_e-\mu_{\nu_e}$, for the neutrino-trapped case in the absence of $\bar{K}$ condensate are depicted in the figure. In neutrino-trapped matter, the in-medium energy of the K^- meson is lower compared with that of neutrino-free matter. This difference in the energies of the K^- meson stems from different behaviors of the meson fields in two cases as is evident from Fig. 1. The threshold densities of K^- condensation in neutrino-free and neutrino-trapped matter are $2.43n_0$ and $3.07n_0$, respectively. In the presence of trapped neutrinos, the onset of K^- condensation is shifted to higher density because the curve representing the difference of electron and neutrino chemical potentials ($\mu_e-\mu_{\nu_e}$) intersects the ω_{K^-} curve at higher density. On the other hand, the threshold condition for $\bar{K}^0$ condensation is always $\omega_{\bar{K}}=0$. Unlike the situation with the K^- meson, we find that the in-medium energy of the $\bar{K}^0$ meson in neutrino-trapped matter is higher than that of the neutrino-free case. The threshold densities for $\bar{K}^0$ condensation are $3.59n_0$ and $3.81n_0$ for neutrino-free and neutrino-trapped matter, respectively. The early appearance of K^- condensate delays the formation of $\bar{K}^0$ condensate in the neutrino-free (-trapped) matter to a higher density. As a result of the presence of neutrinos, the shift in the threshold density of $\bar{K}^0$ condensation is smaller with respect to the neutrino-free case than the corresponding situation with K^- condensation. We note that the difference between the energies of $\bar{K}^0$ and K^- in the neutrino-trapped case is smaller than that of the neutrino-free case because the isovector potential is smaller in the former case. Threshold densities of $\bar{K}$ condensation for the GM1 set and other values of $U_{\bar{K}}(n_0)$ are given in Table III. The values given in the parentheses correspond to neutrino-free matter.

The populations of various particles in proto(neutron) star matter with K^- and $\bar{K}^0$ condensation for $U_{\bar{K}}=-160$ MeV

TABLE III. The maximum masses M_{max} and their corresponding central densities $u_{cent}=n_{cent}/n_0$ for neutrino-trapped nucleon-only (np) star matter and for stars with further inclusion of hyperons (npH) are given below. The lepton fraction in neutrino-trapped matter is $Y_{L_e}=Y_e+Y_{\nu_e}=0.4$. The results are for the GM1 set. For protoneutron star matter with nucleons and antikaons ($np\bar{K}$), the critical densities for K^- and $\bar{K}^0$ condensation, $u_{cr}(K^-)$ and $u_{cr}(\bar{K}^0)$, and also the results for M_{max} and u_{cent} at various values of the antikaon potential depth $U_{\bar{K}}$ (in MeV) at the saturation density are given. The values in the parentheses are for the neutrino-free matter relevant to neutron stars.

	$U_{\bar{K}}$	$u_{cr}(K^-)$	$u_{cr}(\bar{K}^0)$	u_{cent}	$M_{max}/M_\odot$
np	-	-	-	5.84 (5.63)	2.283 (2.364)
	-100	4.40 (3.45)	5.71 (5.51)	5.68 (5.17)	2.258 (2.211)
	-120	3.90 (3.05)	5.03 (4.83)	5.57 (5.19)	2.218 (2.077)
$np\bar{K}$	-140	3.45 (2.71)	4.39 (4.19)	5.33 (4.75)	2.134 (1.856)
	-160	3.07 (2.43)	3.81 (3.59)	4.89 (3.59)	1.970 (1.551)
	-180	2.74 (2.19)	3.31 (3.07)	4.74 (3.09)	1.686 (1.217)
npH	-	-	-	5.66 (5.16)	2.043 (1.789)

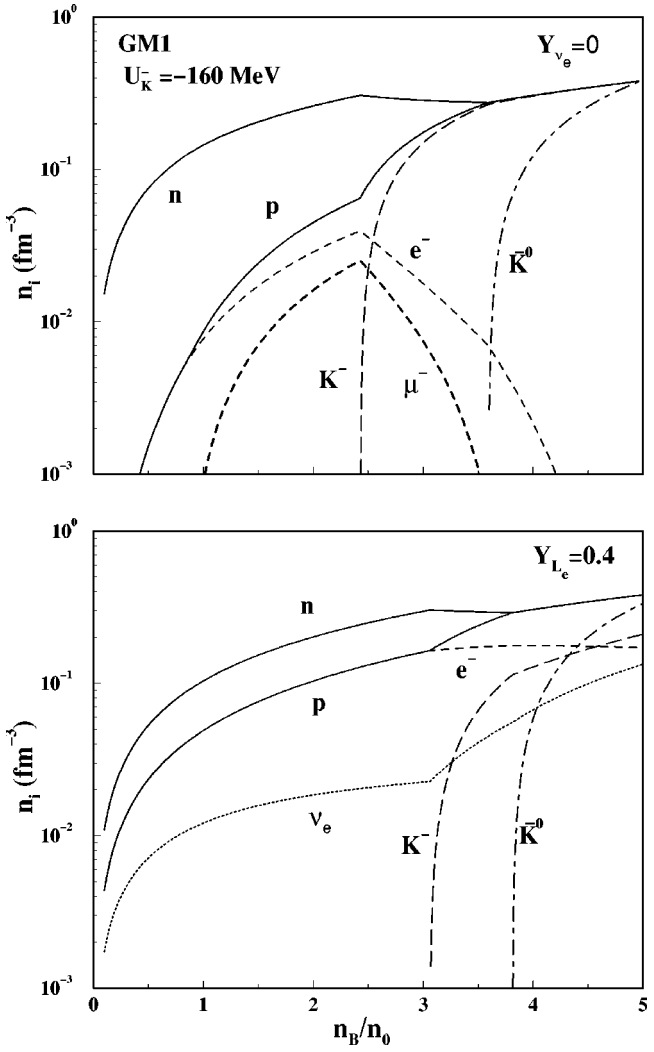

FIG. 4. The proper number densities n_i of various compositions in (proto)neutron star matter including antikaon condensates in the GM1 model. The results are for neutrino-free matter (top panel) and neutrino-trapped matter (bottom panel). The $\bar{K}$ optical potential at normal nuclear matter density is $U_{\bar{K}}^{-}=-160$ MeV.

are shown in Fig. 4. In the top panel we exhibit the particle abundances of neutrino-free star matter. In neutrino-free matter, once K^- condensate sets in at $2.43n_0$, it rapidly increases with density, replacing the leptons in maintaining the charge neutrality. The proton density becomes equal to the K^- condensate density because of the charge neutrality. With the onset of $\bar{K}^0$ condensate at $3.59n_0$, the neutron and proton abundances become identical, resulting in a symmetric matter of nucleons and antikaons [18]. In the previous calculation of K^- condensation in neutron star matter [4,8,13], it was found that protons were more abundant than neutrons at higher densities. In the bottom panel of Fig. 4, we show the particle fractions with both K^- and $\bar{K}^0$ condensates for neutrino-trapped matter. We have a somewhat different picture here. With the formation of K^- condensate at $3.07n_0$, it cannot replace electrons totally like the neutrino-free case because of the constraint $Y_{L_e}=0.4$ in the system. At higher baryon densities, the electron density slowly falls and the density of K^- condensate becomes higher than the electron density. As soon as $\bar{K}^0$ condensate is formed at $3.81n_0$, the neutron density becomes equal to the proton density and it continues in the high density regime. Like the neutrino-free case (top panel), neutrino-trapped matter becomes symmetric nuclear matter just with the formation of $\bar{K}^0$ condensate. On the other hand, the density of $\bar{K}^0$ condensate increases with baryon density uninterruptedly and even becomes larger than the density of K^- condensate beyond $\sim 4n_0$. As a result, the ρ-meson field becomes zero at the onset of $\bar{K}^0$ condensation and then bounces back (see Fig. 1) unlike the situation in neutrino-free matter where the isovector field is zero at and beyond the onset of $\bar{K}^0$ condensation. It is interesting to note that beta-equilibrated and charge-neutral neutrino-trapped matter is mainly dominated by $\bar{K}^0$ condensate than K^- condensate after the formation of $\bar{K}^0$ condensate.

The equation of state or the pressure (P) versus energy density (ϵ) for neutrino-free and neutrino-trapped matter is displayed in Fig. 5. The top panel represents nucleon-only matter. Here, the dashed line stands for the neutrino-trapped case and the solid line implies the neutrino-free case. The overall EOS of neutrino-trapped matter is softer compared with that of neutrino-free matter. It is due to the delicate interplay of the contributions of the symmetry and lepton terms to the energy density (pressure) in both cases. As trapped neutrinos leave the system, the conversion of protons to neutrons increases the energy density (pressure) more than it is decreased by the loss of neutrinos. This scenario is changed in the presence of antikaon condensation. This is demonstrated in the bottom panel of Fig. 5 with $U_{\bar{K}}^{-}=-160$ MeV. We find that the overall EOS of neutrino-trapped matter is now stiffer than that of neutrino-free matter. During deleptonization, the contribution of the nuclear symmetry term to the energy density (pressure) does not change at all in this case with K^- and $\bar{K}^0$ condensate at higher densities. This happens because both neutrino-free and neutrino-trapped matter become isospin-saturated nuclear matter at the onset of $\bar{K}^0$ condensation. Such a situation does not arise for (proto)neutron star matter with K^- condensate because more protons than neutrons are favored by K^- condensate due to the charge neutrality. It is important to note here that the incompressibility of matter ($K=9dP/dn_B$) becomes negative with the formation of $\bar{K}$ condensates in neutrino-free matter as is evident from Fig. 5. To get rid of those unphysical regions from the energy density versus pressure curve and maintain a positive incompressibility, a Maxwell construction is done here. This implies a first order phase transition. We note that the phase transition is of second order in the neutrino-free case for smaller values of the antikaon potential and in the neutrino-trapped case for all values of the antikaon potential. It is worth mentioning here that the condensation of K^- meson was treated as a first order phase transition using Gibbs criteria [15]. In this case, matter would have a normal phase of baryons and leptons at low density followed by a mixed phase of K^- condensate and baryons and a pure phase of K^- condensate at higher densities. This scenario would be more complicated with the

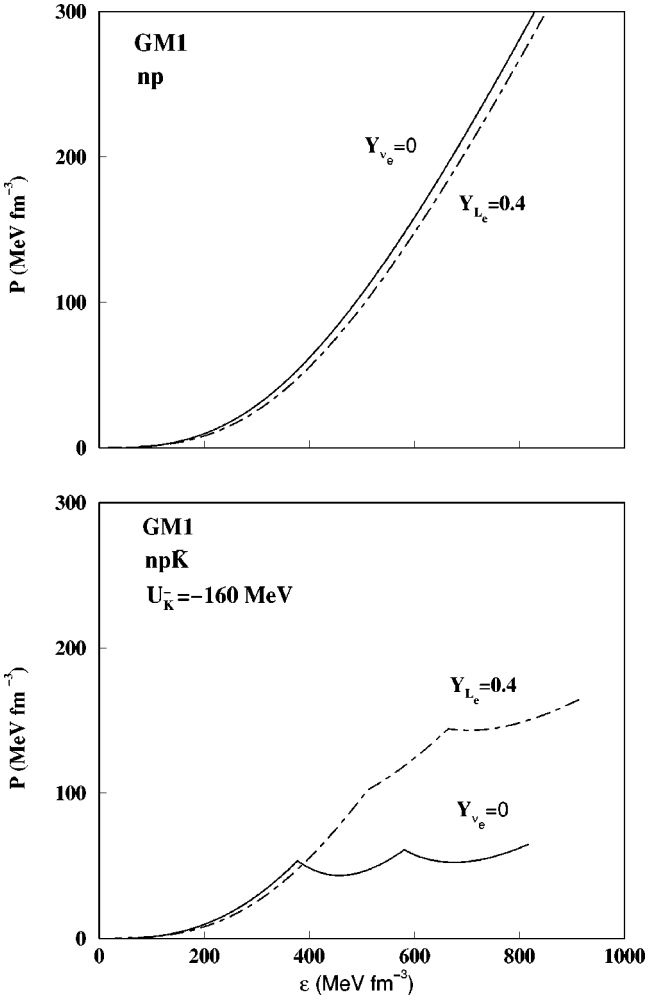

FIG. 5. The equation of state, pressure P vs energy density ε in the GM1 set. The results are for nucleon-only (np) (proto)neutron star matter (top panel) and with further inclusion of K^- and $\overline{K}^0$ condensation (bottom panel) calculated with the antikaon optical potential depth at normal nuclear matter density of $U_{\overline{K}}=-160$ MeV. The equation of state for neutrino-free matter is denoted by the solid line and that of neutrino-trapped matter by the dashed line.

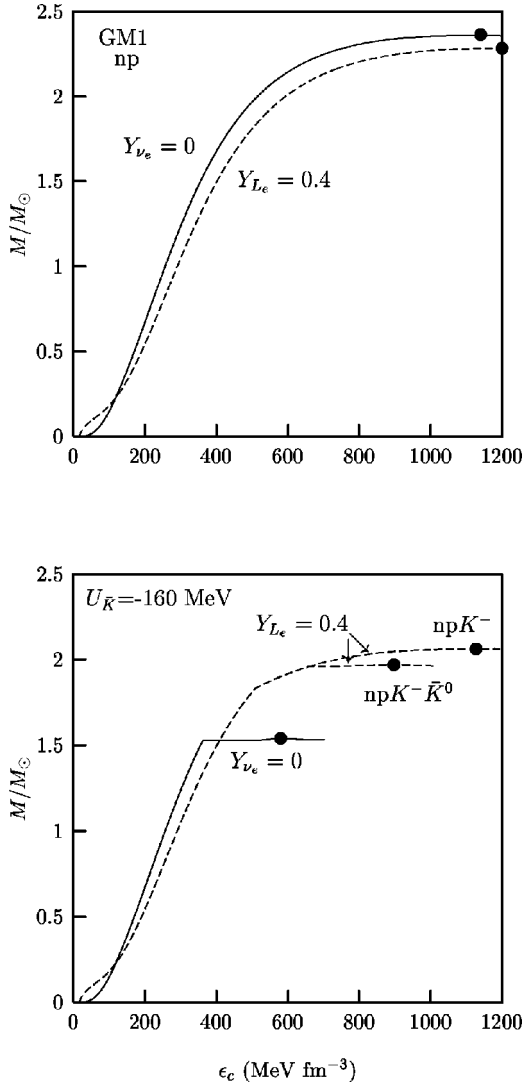

FIG. 6. The (proto)neutron star mass sequences are plotted with central energy density in the GM1 set for the antikaon optical potential depth of $U_{\overline{K}}=-160$ MeV. The star masses of nucleon-only matter and with further inclusion of K^- and $\overline{K}^0$ condensation are shown in the top and bottom panel, respectively. The solid curve corresponds to the neutrino-free case whereas the dashed curve represents the neutrino-trapped case. The solid circles correspond to the maximum masses.

further appearance of $\overline{K}^0$ condensate because K^- and $\overline{K}^0$ condensation have to be treated as two separate first order phase transitions. Therefore, the treatment of such a problem is beyond the scope of this work.

Now we present the results of static structures of (proto-)neutron stars calculated using Tolmann-Oppenheimer-Volkov (TOV) equations. The static (proto)neutron star sequences representing the stellar masses $M/M_\odot$ and the corresponding central energy density ε_c are shown in Fig. 6 for the GM1 set. The neutrino-free stars are denoted by the solid lines and the neutrino trapped stars are represented by the dashed lines in Fig. 6. The ''conventional'' scenario, i.e., stars made of nucleons, leptons, and no $\overline{K}$ condensation, is shown in the top panel. The maximum masses (M_{max}) and central densities (n_c) of the neutrino trapped and neutrino-free stars are, respectively, given by $2.283(2.364)M_\odot$ and $5.84(5.63)n_0$. The protoneutron star has a smaller mass compared with that of the neutron star because the EOS is softer in the former case. In the bottom panel, the masses of (proto)neutron stars with both K^- and $\overline{K}^0$ condensation and $U_{\overline{K}}(n_0)=-160$ MeV are plotted (the dashed curve with the label $npK^-\overline{K}^0$) with central energy density. In this case, the maximum masses of the (proto)neutron stars are $1.97(1.55)M_\odot$ corresponding to the central densities $4.89(3.59)n_0$, respectively. For the mass sequence of neutron stars containing both condensates, there is a flat region extending from the central density (central energy density) $2.36n_0$ (365.13 MeV fm^{-3}) to $3.36n_0$ (518.73 MeV fm^{-3}). That region corresponds to the constant pressure region in the equation of state. This is the signature of the Maxwell construction. We note that the masses and radii of

neutron stars are constant in the flat region. However, the maximum mass for the neutron star lies above this flat region, i.e., at the central density $3.59n_0$. It is worth mentioning here that the Maxwell construction has its limitations. In the Maxwell construction case, the thermodynamical variables such as the pressure and chemical potential are not a continuously increasing function of density. Also, there is a mechanical instability in the flat region of the mass versus central energy density curve in the Maxwell construction case. In that region, the stability condition $dM/d\varepsilon_c > 0$ is not satisfied. Therefore, no star with central density falling in the mixed phase region will be stable for the Maxwell construction case.

We note here that the maximum masses of the (proto)neutron stars including antikaon condensates are smaller than those of the ''conventional'' scenario. This can be attributed to the softening of the EOS due to the presence of $\overline{K}$ condensates. In the previous calculations including K^- condensate [4,6,7,13–15] this kind of softening in the EOS and reduction in the maximum mass of the star were observed. The net result of K^- condensation is that the maximum mass stars contain more protons than neutrons at higher densities. Brown and Bethe [2,3] called those stars ''nuclear matter'' stars rather than neutron stars. In the bottom panel, we also plot the sequence of protoneutron star masses calculated with only K^- condensation. This is shown by the dashed curve labeled by npK^-. In the neutrino-trapped case, the additional softening in the EOS due to $\overline{K}^0$ condensate results in a smaller maximum mass for the star compared with the corresponding situation with only K^- condensate. In the bottom panel and Table III, we find that the threshold density of $\overline{K}^0$ condensation for the neutrino trapped case lies well inside the central density of the maximum mass star. This implies that a significant region of the protoneutron star may contain $\overline{K}^0$ condensate along with K^- condensate. In the neutrino-free case, the maximum mass of the star including both antikaon condensates is not modified appreciably due to $\overline{K}^0$ condensate with respect to the situation calculated with only K^- condensate because the threshold density of $\overline{K}^0$ condensation coincides with the central density of the maximum mass star in the former case. It is interesting to note that the maximum mass stars in the presence of K^- and $\overline{K}^0$ condensate contain exactly equal the number of protons and neutrons at higher densities. Therefore, those stars may be called ''symmetric nuclear matter'' stars. We have also calculated the maximum masses and central densities of the (proto)neutron stars for the GM1 set and other values of $U_{\overline{K}}(n_0)$ and those are tabulated in Table III. The values given in the parentheses correspond to neutrino-free matter. It is to be noted here that the maximum mass of the neutron star in the GM1 set and with $U_{\overline{K}}(n_0) = -180$ MeV is smaller than the precise observational lower limit of $1.44M_\odot$ imposed by the larger mass of the binary pulsar PSR 1913 + 16 [29]. Therefore, such a softer EOS is ruled out by the observation.

In a recent calculation for neutrino-free matter including $\overline{K}$ condensates, it has been noted that the critical densities of antikaon condensation are sensitive to the nuclear equation of state apart from its dependence on the antikaon potential depth [18]. Therefore, we also study the formation of $\overline{K}$ condensates in neutrino-trapped matter using a softer EOS. In this calculation, the model Lagrangian density contains a nonlinear ω-meson term [30,31] besides the self-interaction term for the scalar meson. The form of the nonlinear ω meson term is

$$\mathcal{L}_{\omega^4} = \frac{1}{4} g_4 (\omega_\mu \omega^\mu)^2. \tag{25}$$

Sugahara and Toki [31] showed that such a model agreed with the relativistic Brückner Hartree-Fock results reasonably well. The parameters of the model were obtained by fitting the experimental data for binding energies and charge radii of heavy nuclei. This set of parameters is known as the TM1 set [31]. The nucleon-meson couplings of the TM1 set are shown in Table I and $g_{\sigma K}$ couplings for various $U_{\overline{K}}(n_0)$ are given in Table II. Now we present the results for the calculation of $\overline{K}$ condensation in neutrino-trapped nucleon-only matter using the TM1 set. The critical densities of $\overline{K}$ condensation and maximum masses of (proto)neutron stars with their corresponding central densities for the TM1 set are shown in Table IV. The values in the parentheses correspond to the neutrino-free cases. Because of the presence of the nonlinear ω meson term, the TM1 set results in a softer EOS than that with the GM1 set. As a result, the critical densities of $\overline{K}$ condensation for the TM1 set are shifted to higher densities compared with those of the GM1 set. It is found that $\overline{K}^0$ condensation is formed inside the maximum mass neutron stars for $|U_{\overline{K}}(n_0)| \geqslant 160$ MeV and inside the maximum mass protoneutron star only for $U_{\overline{K}}(n_0) = -180$ MeV in the TM1 set. It is important to note that the phase transition is of second order for all values of the antikaon potential depth in the TM1 set [18].

TABLE IV. Same as Table III, but for the TM1 set.

	$U_{\overline{K}}$	$u_{cr}(K^-)$	$u_{cr}(\overline{K}^0)$	u_{cent}	$M_{max}/M_\odot$
np	-	-	-	6.14 (5.97)	2.099 (2.179)
	-100	6.80 (4.15)	11.61 (11.12)	6.14 (5.67)	2.099 (2.142)
	-120	5.63 (3.55)	9.38 (9.13)	6.13 (5.55)	2.098 (2.083)
$np\overline{K}$	-140	4.68 (3.05)	7.53 (7.43)	6.02 (5.65)	2.087 (1.986)
	-160	3.92 (2.67)	6.04 (5.99)	5.92 (6.37)	2.058 (1.857)
	-180	3.34 (2.37)	4.85 (4.81)	5.72 (6.01)	1.985 (1.641)
npH	-	-	-	5.75 (4.88)	1.918 (1.733)

Now we discuss situations when hyperons are included in the calculation in addition to nucleons. It was noted earlier that the presence of hyperons delayed the onset of $\overline{K}$ condensation to a much higher density [4,8,12–14,18]. Since the core of a (proto)neutron star may be hyperon rich, we include the hyperon-hyperon interaction in addition to the hyperon-nucleon interaction in our calculation. This is ac-

counted for by considering two additional hidden-strangeness mesons—the scalar meson $f_0(975)$ (denoted by σ^*) and the vector meson $\phi(1020)$. The vector coupling constants for hyperons are determined from the SU(6) symmetry as

$$\frac{1}{2}g_{\omega\Lambda}=\frac{1}{2}g_{\omega\Sigma}=g_{\omega\Xi}=\frac{1}{3}g_{\omega N},$$

$$\frac{1}{2}g_{\rho\Sigma}=g_{\rho\Xi}=g_{\rho N}, \quad g_{\rho\Lambda}=0,$$

$$2g_{\phi\Lambda}=2g_{\phi\Sigma}=g_{\phi\Xi}=-\frac{2\sqrt{2}}{3}g_{\omega N}. \tag{26}$$

The scalar meson (σ) coupling to hyperons is obtained from the potential depth of a hyperon (Y) in saturated nuclear matter:

$$U_Y^N(n_0)=-g_{\sigma Y}\sigma+g_{\omega Y}\omega_0. \tag{27}$$

The analysis of energy levels in Λ hypernuclei suggests a well depth of Λ in symmetric matter, $U_\Lambda^N(n_0)=-30$ MeV [32,33]. On the other hand, recent analysis of a few Ξ-hypernuclei events predicts a Ξ well depth of $U_\Xi^N(n_0)=-18$ MeV [34,35]. However, the situation for the Σ potential in normal matter is very unclear. The only known bound Σ-hypernuclei is the light system ${}^4_\Sigma$He [36]. The most updated analysis of Σ^- atomic data indicates a strong isoscalar repulsion in the Σ–nuclear-matter interaction [23]. Therefore, we use a repulsive Σ well depth of $U_\Sigma^N(n_0)=30$ MeV [23] in our calculation.

The σ^*-Y coupling constants are obtained by fitting them to a well depth $U_Y^{(Y')}(n_0)$ for a hyperon (Y) in a hyperon (Y') matter at nuclear saturation density [14,20]. It is given as

$$U_\Xi^{(\Xi)}(n_0)=U_\Lambda^{(\Xi)}(n_0)=2U_\Xi^{(\Lambda)}(n_0)=2U_\Lambda^{(\Lambda)}(n_0)$$
$$=-40 \text{ MeV}. \tag{28}$$

It is to be noted that nucleons do not couple to the strange mesons, i.e., $g_{\sigma^*N}=g_{\phi N}=0$.

The strange meson fields also couple with (anti)kaons. Following Ref. [14], the σ^*-K coupling constant is determined from the decay of $f_0(925)$ as $g_{\sigma^*K}=2.65$, whereas the vector ϕ-meson coupling with (anti)kaons is obtained from the SU(3) relation as $\sqrt{2}g_{\phi K}=6.04$.

Switching off Y-Y interactions and antikaon condensation, we study neutrino-free (-trapped) hyperon matter for the GM1 and TM1 set and for the above choices of hyperon-nucleon coupling constants. Here, we find that the Λ hyperon is the first strange baryon to appear in neutrino-free (-trapped) matter. It is closely followed by Ξ^- hyperons. Because of the repulsive Σ-nucleon interaction, Σ hyperons do not appear in the systems. With the appearance of hyperons, equations of state in neutrino-free (-trapped) matter are softer compared with those of nucleon-only matter excluding $\bar{K}$ condensation. The maximum masses and their corresponding central densities are given in the last rows of Tables III and IV. The values in the parentheses correspond to the neutrino-free cases. Like the situations with antikaon condensates in neutrino-free (-trapped) nucleon-only matter, the maximum mass in neutrino-trapped hyperon matter is larger than that of the corresponding neutrino-free case as found in the previous calculations [4,8,13].

Now we study the formation of antikaon condensation in neutrino-free (-trapped) matter including the hyperon-hyperon interaction for the GM1 set. Earlier we have found that a softer EOS shifts the threshold densities of antikaon condensations to higher densities. Also, the presence of hyperons, which make the EOS softer, delays the onsets of $\bar{K}$ condensation to higher densities [4,8,13,14,18]. In this case, we find that antikaon condensation does not occur even at densities as large as $7.5n_0$ in neutrino-free (-trapped) hyperon matter for $|U_{\bar{K}}(n_0)|<160$ MeV. Antikaon condensates appear in hyperon rich matter with and without neutrinos for $|U_{\bar{K}}(n_0)|\geqslant 160$ MeV. The particle abundances in the presence of hyperons and antikaon condensations are shown in Fig. 7 for $U_{\bar{K}}=-160$ MeV. The top panel depicts the neutrino-free case whereas the neutrino-trapped case is shown in the bottom panel. Here, we note that K^- and $\bar{K}^0$ condensation sets in at $2.48(3.34)n_0$ and $4.06(4.18)n_0$ for neutrino-free (-trapped) matter, respectively. Also, we find that only Λ hyperons appear both in neutrino-free and -trapped matter. The Σ's are excluded from the systems because of the repulsive Σ-nucleon interaction. On the other hand, the early appearance of K^- condensation in neutrino-free (-trapped) matter suppresses the appearance of Ξ^- hyperons because it is energetically favorable for K^- condensate to maintain charge neutrality in the systems. It is worth mentioning here that $\bar{K}$ condensates play a more dominant role than hyperons in determining various properties of the (proto)neutron stars in this case.

In Fig. 8, we display the EOS (P vs ϵ) in the top panel and the mass sequence of the (proto)neutron stars in the bottom panel for the GM1 set and $U_{\bar{K}}(n_0)=-160$ MeV. Neutrino-trapped matter has a stiffer EOS than that of the corresponding neutrino-free matter. The maximum masses and their central densities for the neutrino-free (-trapped) cases are $1.57(1.98)M_\odot$ and $4.48(5.24)n_0$, respectively.

The delayed neutrino emission and possible black hole formation in the context of SN 1987A had been extensively discussed by Brown and Bethe [2,3]. This problem was also studied by several authors using dynamical models [37,38]. Assuming that SN 1987A has collapsed into a black hole, Brown and Bethe estimated the gravitational mass for the compact remnant in it to be $1.56M_\odot$ from the Ni production. This maximum mass of the cold compact object is known as the Bethe-Brown limit [3]. They argued that progenitor stars having masses in the range $(18–30)M_\odot$ would first explode as supernovas and later the compact objects go into low mass black holes returning matter to the galaxy [2,3].

In previous studies [2–4], it was shown that the proto-neutron stars become unstable after deleptonization and cooling. The metastability occurs when an exotic form of matter such as hyperons or antikaon condensates, appears during the

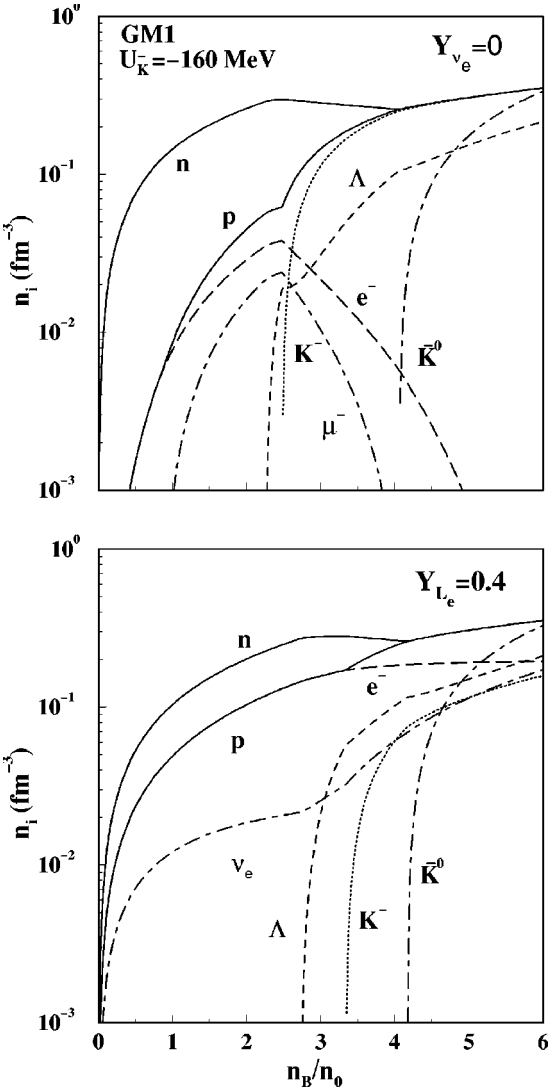

FIG. 7. Same as Fig. 4, but for hyperon matter including K^- and $\bar{K}^0$ condensation in the GM1 set. The results are for the neutrino-free case (top panel) and the neutrino-trapped case (bottom panel).

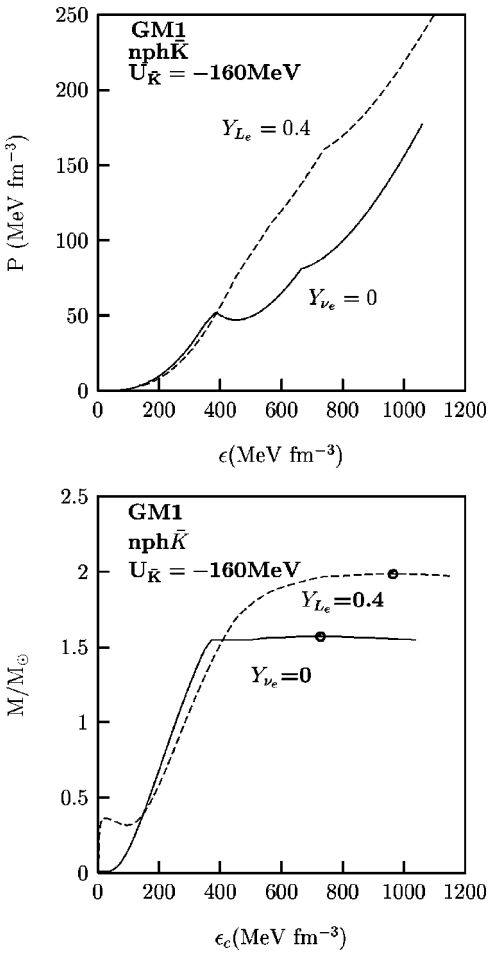

FIG. 8. The equations of state (top panel) for neutrino-free (-trapped) hyperon matter including antikaon condensates with energy density in the GM1 set. The mass sequences (bottom panel) of the (proto)neutrino stars including antikaon condensates are shown with central energy density in the GM1 set. The calculations are performed for $U_{\bar{K}}(n_0) = -160$ MeV. The solid and dashed lines correspond to the neutrino-free and -trapped cases, respectively. The solid circles correspond to the maximum masses.

evolution of the protoneutron stars. Brown and Bethe exploited the idea of the formation of K^- condensation in dense nuclear matter [3] to understand the metastability of the compact object during the evolution of the protoneutron stars to low mass black holes. In the ''conventional'' scenario without antikaon condensation or hyperons, the ''window,'' i.e., the difference of the maximum masses in neutrino-free and neutrino-trapped matter consisting of nucleons, is small. Later it was shown that the inclusion of thermal pressure could raise the maximum mass of the protoneutron star slightly above that of the neutron star [4]. However, there is a different scenario with K^- condensation as noted by various authors [2–4,7]. They found that mostly the lepton pressure could stabilize a larger mass in the neutrino-trapped case during the evolution. In our calculation with nucleons, leptons, and K^- condensation, the ''window'' is $\sim 0.5 M_\odot$ for the GM1 set and an antikaon potential depth of -160 MeV. With further inclusion of $\bar{K}^0$ condensate, high density matter contains exactly as many protons as neutrons. As a result, high density matter remains symmetric nuclear matter even after the deleptonization and cooling. The presence of both condensates stabilizes the larger maximum mass of the protoneutron star for short times. In this case, we obtain the maximum mass window of $\sim 0.4 M_\odot$. In our model calculation with the GM1 set and the antikaon potential of $U_{\bar{K}}(n_0) = -160$ MeV, the protoneutron stars consisting of nucleons, leptons, and K^- and $\bar{K}^0$ condensates have a maximum mass $\sim 2 M_\odot$ which could be stable during the deleptonization and cooling. As the trapped neutrinos leave the system, the lepton pressure in the core decreases. At the same time, the core of the nascent star is heated up and attains a higher value of entropy [39]. Recently, it was shown by Pons *et al.* [16] that this thermal effect on the maximum mass is comparable to that of the trapped neutrinos. As a consequence, compact object would be stable for much longer duration. The inclusion of the thermal pressure in the calculation would again stabilize an additional mass of $\sim 0.1 M_\odot$. As the system cools down, the compact object

with a maximum mass $\geqslant 2M_{\odot}$, which would be stable for short times in our calculation, is larger than that of the stable cold mass and Bethe-Brown limit ($1.56M_{\odot}$). Consequently, it would collapse into a low mass black hole. We retain the same qualitative feature of metastability of the protoneutron stars including hyperons along with antikaon condensation.

IV. SUMMARY AND CONCLUSIONS

We have studied antikaon condensation, putting emphasis on the formation of $\overline{K^0}$ condensation in neutrino-trapped nuclear and hyperon matter within a relativistic mean field model. The baryon-baryon and (anti)kaon-baryon interactions are treated on the same footing in this work. Those interactions are mediated by the exchange of mesons. Two different model Lagrangians are adopted in this calculation. The model Lagrangian, which contains the scalar self-interaction term, is characterized by the GM1 parameter set. Besides the scalar self-interaction term, the other model Lagrangian includes the nonlinear ω-meson term and the corresponding parameter set is denoted by the TM1 set. It is found that the threshold densities of antikaon condensation are sensitive to the equation of state and the antikaon potential in normal nuclear matter. The calculations performed with the GM1 and TM1 sets show that K^- condensation always happens earlier than $\overline{K^0}$ condensation. The threshold densities of $\overline{K}$ condensation in the TM1 set are higher than those of the GM1 set because the equation of state is softer in the former case. It is found that the threshold densities of antikaon condensation in neutrino-trapped nucleon-only matter are higher than those of the corresponding neutrino-free case. In the presence of neutrinos, the shift in the threshold density of K^- condensation with respect to the neutrino-free case is higher than that of $\overline{K^0}$ condensation.

With the onset of $\overline{K^0}$ condensation, abundances of neutrons and protons become equal and the density of $\overline{K^0}$ condensate increases rapidly and becomes larger than that of K^- condensate in neutrino-trapped nuclear matter. On the contrary, neutrino-free nuclear matter is not only symmetric in neutrons and protons but also in K^- and $\overline{K^0}$ mesons at high density. Therefore, it is possible that $\overline{K^0}$ condensate in neutrino-trapped matter would play a dominant role over K^- condensate at higher densities. Unlike the situation in neutrino-free nuclear matter, K^- mesons in the condensate replace electrons partially in neutrino-trapped matter because of the lepton number constraint in the system. The presence of K^- and $\overline{K^0}$ condensate in neutrino-trapped nuclear matter makes the overall equation of state softer compared with the situation without antikaon condensate. We find that $\overline{K^0}$ condensate is formed well inside the maximum mass proto-neutron stars for higher values of the antikaon potential in the calculation using the TM1 set. On the other hand, the calculation with the GM1 set implies that $\overline{K^0}$ condensate occupies a significant region of the maximum mass stars for rather smaller values of the antikaon potential. In the presence of hyperons, antikaon condensate is formed for large values of $|U_{\overline{K}}| \geqslant 160$ MeV in the GM1 set. In this case, it is found that only Λ hyperons appear in neutrino-free (-trapped) hyperon matter. Therefore K^- and $\overline{K^0}$ condensates may play the most dominant role in determining various gross properties of (proto)neutron stars than hyperons.

We have reexamined the scenario of the metastability of protoneutron stars and their evolution to low mass black holes in the context of the calculation of $\overline{K^0}$ condensation along with K^- condensation in neutrino-free (-trapped) nuclear and hyperon matter. It is found that the maximum mass of a protoneutron star is larger than that of the corresponding neutron star and also the Bethe-Brown limit of $1.56M_{\odot}$ for a neutron star. Therefore, the protoneutron star would be stable during deleptonization and cooling and later may collapse into a low mass black hole.

ACKNOWLEDGMENT

We acknowledge many fruitful discussions with Subrata Pal.

[1] S.E. Woosley and T.A. Weaver, Annu. Rev. Astron. Astrophys. **24**, 205 (1986).
[2] G.E. Brown, Nucl. Phys. **A574**, 217c (1994).
[3] G.E. Brown and H.A. Bethe, Astrophys. J. **423**, 659 (1994).
[4] M. Prakash, I. Bombaci, M. Prakash, P.J. Ellis, J.M. Lattimer, and R. Knorren, Phys. Rep. **280**, 1 (1997).
[5] D.B. Kaplan and A.E. Nelson, Phys. Lett. B **175**, 57 (1986); A.E. Nelson and D.B. Kaplan, *ibid.* **192**, 193 (1987).
[6] G.E. Brown, K. Kubodera, M. Rho, and V. Thorsson, Phys. Lett. B **291**, 355 (1992).
[7] V. Thorsson, M. Prakash, and J.M. Lattimer, Nucl. Phys. **A572**, 693 (1994).
[8] P.J. Ellis, R. Knorren, and M. Prakash, Phys. Lett. B **349**, 11 (1995).
[9] G.E. Brown, C.-H. Lee, M. Rho, and V. Thorsson, Nucl. Phys. **A567**, 937 (1994); C.-H. Lee, H. Jung, D.-P. Min, and M. Rho, Phys. Lett. B **326**, 14 (1994).
[10] G.Q. Li, C.-H. Lee, and G.E. Brown, Phys. Rev. Lett. **79**, 5214 (1997); Nucl. Phys. **A625**, 372 (1997).
[11] C.-H. Lee, G.E. Brown, D.-P. Min, and M. Rho, Nucl. Phys. **A585**, 401 (1995).
[12] T. Muto, Prog. Theor. Phys. **89**, 415 (1993).
[13] R. Knorren, M. Prakash, and P.J. Ellis, Phys. Rev. C **52**, 3470 (1995).
[14] J. Schaffner and I.N. Mishustin, Phys. Rev. C **53**, 1416 (1996).
[15] N.K. Glendenning and J. Schaffner-Bielich, Phys. Rev. C **60**, 025803 (1999).
[16] J.A. Pons, S. Reddy, P.J. Ellis, M. Prakash, and J.M. Lattimer, Phys. Rev. C **62**, 035803 (2000).
[17] M. Lutz, A. Steiner, and W. Weise, Nucl. Phys. **A547**, 755 (1994).
[18] S. Pal, D. Bandyopadhyay, and W. Greiner, Nucl. Phys. **A674**, 553 (2000).

[19] B.D. Serot and J.D. Walecka, Adv. Nucl. Phys. **16**, 1 (1986).
[20] J. Schaffner, C.B. Dover, A. Gal, D.J. Millener, C. Greiner, and H. Stöcker, Ann. Phys. (N.Y.) **235**, 35 (1994).
[21] J. Boguta and A.R. Bodmer, Nucl. Phys. **A292**, 413 (1977).
[22] N.K. Glendenning and S.A. Moszkowski, Phys. Rev. Lett. **67**, 2414 (1991).
[23] E. Friedman, A. Gal, and C.J. Batty, Nucl. Phys. **A579**, 518 (1994); C.J. Batty, E. Friedman, and A. Gal, Phys. Rep. **287**, 385 (1997).
[24] E. Friedman, A. Gal, J. Mareš, and A. Cieplý, Phys. Rev. C **60**, 024314 (1999).
[25] V. Koch, Phys. Lett. B **337**, 7 (1994).
[26] T. Waas and W. Weise, Nucl. Phys. **A625**, 287 (1997).
[27] T. Cohen, Phys. Rev. C **39**, 2285 (1989).
[28] T. Barnes and E.S. Swanson, Phys. Rev. C **49**, 1166 (1994).
[29] J.M. Weisberg and J.H. Taylor, Phys. Rev. Lett. **52**, 1348 (1984).
[30] A.R. Bodmer, Nucl. Phys. **A526**, 703 (1991).
[31] Y. Sugahara and H. Toki, Nucl. Phys. **A579**, 557 (1994).
[32] R.E. Chrien and C.B. Dover, Annu. Rev. Astron. Astrophys. **39**, 113 (1989).
[33] C.B. Dover and A. Gal, Prog. Part. Nucl. Phys. **12**, 171 (1984).
[34] T. Fakuda *et al.*, Phys. Rev. C **58**, 1306 (1998).
[35] P. Khaustov *et al.*, Phys. Rev. C **61**, 054603 (2000).
[36] R.S. Hayano *et al.*, Phys. Lett. B **231**, 355 (1989).
[37] W. Keil and H.-Th. Janka, Astron. Astrophys. **296**, 145 (1995).
[38] T.W. Baumgarte, H.-Th. Janka, W. Keil, S.L. Shapiro, and S.A. Teukolsky, Astrophys. J. **468**, 823 (1996).
[39] A. Burrows and J.M. Lattimer, Astrophys. J. **307**, 178 (1986).